



ORIGINAL ARTICLE

Nickel oxide nanoparticles increase α -synuclein amyloid formation and relevant overexpression of inflammatory mediators in microglia as a marker of Parkinson's disease



Xidong Li^a, Qiushi Li^a, Yanhui Zhang^a, Yang Bai^a, Yue Cao^a, Yang Yang^b, Lie Zang^c, Meiyi Huang^a, Rubo Sui^{a,*}

^a Department of Neurology, The First Affiliated Hospital of Jinzhou Medical University, Jinzhou 121099, China

^b Jinzhou Medical University, Jinzhou 121001, China

^c School of Nursing, Jinzhou Medical University, Jinzhou 121099, China

Received 30 May 2021; accepted 8 August 2021

Available online 12 August 2021

KEYWORDS

α -Synuclein;
Amyloid;
Protein aggregation;
Nickel oxide;
Nanoparticle;
Neurotoxicity

Abstract The study of protein aggregation has received increasing attention owing to their potential role development of neuroadaptive disease. Elsewhere, the use of nanoparticles (NPs) including nickel oxide (NiO) in medicine can result in the interaction of NPs with proteins and exert a toxic effect. Thus, this study was aimed to examine the effects of synthesized NiO NPs via thermal decomposition method on the structural and kinetic characteristics of α -synuclein-protein fibrillization through thioflavin T (ThT) fluorescence, Transmission electron microscopy (TEM), Congo red adsorption, and far-UV circular dichroism (CD) analysis. Also, the increased cytotoxicity of α -synuclein amyloids formed in the presence of NiO NPs was explored by evaluation of oxidative stress and expression of inflammatory and apoptotic mediators in microglia cells as determined by reactive oxygen species (ROS), superoxide dismutase (SOD) and catalase (CAT) activities, and quantitative real-time PCR (qRT-PCR) assays. The obtained results indicated that the fabricated NiO NPs with a dominant average size of about 50 nm led to the secondary structural changes of α -synuclein and accelerated the protein amyloid formation through a significant increase in the k_b and k_a parameters as the homogeneous nucleation rate constant and the secondary rate constant, respectively. Also, it was shown that α -synuclein amyloid aged in the presence of NiO NPs

* Corresponding author at: Department of Neurology, The First Affiliated Hospital of Jinzhou Medical University, No 2. Section5 Renmin Street, Jinzhou 121099, China.

E-mail address: rsui.jmu@yahoo.com (R. Sui).

Peer review under responsibility of King Saud University.



significantly enhanced α -synuclein amyloid -induced cytotoxicity through production of high level of ROS, deactivation of SOD and CAT, overexpression of inflammatory [tumor necrosis factor- α (TNF α), interleukin-1 (IL-1), interleukin-1 β (IL-1 β)] and apoptotic [B-cell lymphoma protein 2 (Bcl-2)-associated X (Bax) and caspase-3] genes over that of α -synuclein amyloid alone in EOC 13.31 mouse microglia cell line. The present work indicated, for the first time, the acceleration effect of NiO NPs against α -synuclein amyloid fibrillization and associated neurotoxicity as a marker of Parkinson's disease.

© 2021 The Author(s). Published by Elsevier B.V. on behalf of King Saud University. This is an open access article under the CC BY-NC-ND license (<http://creativecommons.org/licenses/by-nc-nd/4.0/>).

1. Introduction

Protein aggregation is the process by which molecules naturally present in the form of monomers or small oligomers in solution bind together to form larger protein networks (Cohen et al., 2012). Abnormal conformational changes of proteins are a key feature of the protein aggregation process (Cohen et al., 2012; Koo et al., 1999). Thus, it is assumed that the natural form of the protein is not prone to accumulation, and in order to begin such a process, the tertiary structure of the protein must first be changed (Wang et al., 2010). Protein aggregation can be an irreversible process resulting from the spontaneous association of several similar protein molecules through intramolecular interactions. Factors affecting protein aggregation are divided into two categories: internal and external. Internal factors include electrical charge, hydrophobicity, amino acid pattern and the tendency to form secondary motifs, and external factors include temperature, pH, ionic strength, metal ions, protein concentration, protein source, additives, contact surfaces, presence of nanoparticles (NPs) (Wang et al., 2010).

Given that NPs is one of the most important factors affecting the formation of amyloid fibers, the presence of NPs can cause significant conformational changes in protein structure (Falahati et al., 2019; Gallardo-Toledo et al., 2020). The presence of NPs applies these changes with different mechanisms (Falahati et al., 2019). Excessively high concentration of NPs usually causes the exposure of hydrophobic residues that lead to the formation of amyloid fibers. Also, high concentration of NPs, such as those for protein concentrations, can increase the kinetic mobility of protein molecules and increase the likelihood of producing amyloid fibers (Falahati et al., 2019). However, low concentration of NPs can provide a high accessible surface area for interaction with proteins and production of early nucleus for protein aggregation (Falahati et al., 2019). The application of NPs has received a great deal of interest in different pharmacological sectors and due to their tiny size, they cannot easily cross the blood brain barrier and interact with proteins (Gallardo-Toledo et al., 2020). One of the interesting NPs in the biomedical field is nickel oxide (NiO) with several effective therapeutic applications such as anti-inflammation (Angajala and Radhakrishnan, 2014), anticancer (Cho et al., 2020), and antibacterial properties (Chaudhary et al., 2015).

However, it has been widely exhibited that NiO NPs can induce some unwanted effects on the cell integrity and protein structures (Gamasae et al., 2020; Hosseinali et al., 2019; Nakhjiri et al., 2020). Although the cytotoxicity of NiO NPs have been well- reported, the effects of these NPs on protein

aggregation and underlying neurotoxicity have not been well understood.

Indeed, many neurovegetative diseases are associated with the formation of protein aggregates called amyloid fibrils (Koo et al., 1999). α -Synuclein with a natively unfolded structure can form cytotoxic amyloid fibrils which are known to be a key factor in the development and spread of neurodegenerative diseases in the brain like Parkinson's disease (PD) (Mehra et al., 2019). For example, it has been shown that amyloid fibrils can play a key role in induction of inflammation in PD (Gustot et al., 2015). Also, microglial inflammation associated with α -synuclein deposition has been detected in the substantia nigra of patients suffering from PD (Croisier et al., 2005).

Interestingly, it has been shown that some NPs such as zero-valent iron NPs (Gilan et al., 2019), zinc oxide NPs (Khodabandeh et al., 2020), and silica NPs (Pang et al., 2021) can trigger α -synuclein fibrillization and associated cytotoxicity. However, it has been shown that some other NPs including cerium oxide NPs (Zand et al., 2019); graphene oxide sheets (Ghaeidamini et al., 2020), and quantum dots NPs (Ghaeidamini et al., 2020) can mitigate the formation of α -synuclein amyloids.

Hence, limited application of some NPs that can trigger α -synuclein aggregation or its cytotoxicity can be of great importance in the control of PD.

Therefore, in this study NiO NPs were synthesized through thermal decomposition and the formation of α -synuclein amyloid and underlying inflammation-mediated cytotoxicity on microglia cells were investigated by different spectroscopic, imaging, cellular and molecular assays.

2. Materials and methods

2.1. Materials

Nickel chloride hexahydrate (NiCl₂·6H₂O), hydrazine monohydrate (N₂H₄·H₂O), α -synuclein, thioflavin T (ThT), and Nile red were purchased from Sigma (St. Louis, MO, USA). Dulbecco's modified Eagle's Medium (DMEM) and fetal bovine serum (FBS) were purchased from Gibco BRL Co. (Grand Island, NY, USA). The other materials were of analytical grades and were purchased from Merck (Darmstadt, Germany).

2.2. Synthesis of NiO NPs by thermal decomposition

NiO NPs were fabricated through thermal decomposition of Ni(OH)₂ as the precursor based on the previous reports with some modifications (Wu et al., 2010; El-Kemary et al., 2013).

$\text{NiCl}_2 \cdot 6\text{H}_2\text{O}$ (0.12 M) solution prepared in ethanol was added to $\text{N}_2\text{H}_4 \cdot \text{H}_2\text{O}$ solution (0.6 M) and the pH was fixed at 12. The solution was mixed, stirred for 5 h at 25 °C, washed with deionized water and acetone, dried in vacuum, and calcined at 400 °C.

2.3. Characterization of synthesized NiO NPs

Transmission electron microscopy (TEM) was used to determine the diameter of synthesized NiO NPs employing a Hitachi S-4800 microscope (200 kV). UV–Vis absorption signal was recorded on a Shimadzu UV spectrophotometer to analyze the absorbance properties of NiO NPs. The Fourier-transform infrared (FT-IR) band was obtained using a JASCO spectrometer to assess the vibrational characteristics of NiO NPs.

2.4. Preparation of samples

α -Synuclein (50 μM) either alone or with a fixed concentration of NiO NPs (10 $\mu\text{g}/\text{mL}$) was dissolved in an aggregation buffer (PBS, pH 7.4, 37 °C) and stirred at 100 rpm for 40 h. This concentration of NiO NPs was chosen based on the optimum concentration of this NPs with no aggregation tendency as determined by dynamic light scattering (DLS) (data not shown). Also, the diluted samples of NiO NPs for spectroscopic and cellular assays did not show any interference with detected spectra and also any significant cytotoxic effect.

2.5. ThT analysis

ThT analysis was done to explore the kinetic of α -synuclein aggregation. 20 μL α -synuclein sample solutions (2 μM), with or without NiO NPs, at different time intervals were mixed with 980 μL ThT working solution (10 μM). The samples were incubated at room temperature for 15 min and ThT fluorescence excitation was then fixed at 480 nm, whereas the emission intensity was read at 485 nm using a Cary Eclipse fluorescence spectrophotometer (Varian, USA). where k_b and k_a as the homogeneous nucleation rate constant and the secondary rate constant, respectively were obtained based on the previous reported equation (Crespo et al., 2016).

2.6. Congo red (CR) analysis

CR absorption analysis was done to further characterize the protein aggregation. 25 μL of fresh CR solution with final concentration of 10 μM were added to 1975 μL of α -synuclein, vortexed, and incubated at room temperature for 45 min. Afterwards, the CR absorption samples were recorded using a Cary UV–Visible Spectrophotometer (Varian, USA).

2.7. Far-UV circular dichroism (CD) analysis

The secondary structural changes of α -synuclein (5 μM) were explored over the wavelength range of 190–260 nm with a J-815 spectrometer (JASCO, Japan). The experiment set up was fixed at bandwidth of 1.0 nm, an interval of 0.1 nm, and a scanning rate of 50 nm/min. All measurements were done

at room temperature and each CD band was reported as the average of five scans.

2.8. TEM analysis

α -Syn aggregates aged for 40 h were removed, diluted, sonicated for 2 min, placed on a carbon-coated copper grid, and air-dried for 30 min. Images were then obtained using a Hitachi S-4800 TEM (200 kV) to observe the morphological changes of amyloid proteins.

2.9. Cell culture

EOC 13.31 mouse microglia were obtained from American Type Culture Collection (USA) and were cultured in DMEM containing FBS (10%), penicillin (100 U/mL), streptomycin (100 mg/mL), and L-glutamine (2 mM) and incubated at 37 °C and 5% CO_2 .

The cells were treated with different α -synuclein samples aged for 100 h in the aggregation condition with or without NiO NPs. In cellular assays the protein stock solutions (50 μM) either alone or with a single concentration of NiO NPs (10 $\mu\text{g}/\text{mL}$) were diluted 10-folds. Therefore, the final concentrations of protein and NiO NPs were 5 μM and 1 $\mu\text{g}/\text{mL}$, respectively.

2.10. MTT assay

The microglia viability was measured by doing MTT assay. Briefly, the cells incubated with different samples as indicated in the previous section for 24 h, were added by MTT. The supernatant was then removed, and DMSO was added (5 min incubation). The absorbance was then read spectrophotometrically at 570 nm by employing a microplate reader.

2.11. Quantitative real-time PCR (qRT-PCR) analysis

After the treatment of microglia, total mRNA was extracted using RNeasy Kit (Invitrogen) cDNA was synthesized by using RevertAid kit (Thermo Fisher) under the protocol's instructions. The mRNA was then quantified by carrying out quantitative real-time PCR (qRT-PCR) by employing ABI 7300 Applied Biosystems (USA) by using Power SYBR Green PCR Master Mix (Applied Biosystems). The primers used for this study are tabulated in Table 1.

2.12. Measurement of reactive oxygen species (ROS) levels

After treating, the cells were added by DCFH-DA (10 μM) for 40 min, harvested, and washed. Fluorescence intensity was then read using a Synergy H4 multimode reader at excitation and emission wavelengths of 485 and 520 nm, respectively.

2.13. Superoxide dismutase (SOD) and catalase (CAT) activity assay

SOD and CAT activities were assessed by commercially available kits (Abcam, UK). The cells as were treated as previously described, homogenized, and centrifuged. The protein sample

Table 1 Primers used for qRT-PCR.

| mRNA | FW | Rev |
|--------------|--------------------------------|--------------------------------|
| TNF α | 5'-AGGCACTCCCCAAAAGATG-3' | 5'-TGAGGGT CTGGGCCATAGAA-3' |
| IL-6 | 5'-AGGGCTCTTCGGCAAATGTA-3' | 5'-GAAGGAATGCCCATTAACAACAA-3' |
| IL-1 β | 5'-GCCCATCCTCTGTGACTCAT-3' | 5'-AGGCCACAGGTATTTTGTGCG-3' |
| Bax | 5'-TTTGCTTCAGGGTTTCATCCA-3' | 5'-CTCCATGTTACTGTCCAGTTCGT-3' |
| Bcl-2 | 5'-CATGTGTGTGGAGAGCGTCAAC-3' | 5'-CAGATAGGCACCCAGGGTGAT-3' |
| Caspase-3 | 5'-CATGGAAGCGAATCAATGGACT-3' | 5'-CTGTACCAGACCGAGATGTCA-3' |
| GAPDH | 5'-TGGTATCGTGGAAGGACTCATGAC-3' | 5'-ATGCCAGTGAGCTTCCCGTTCAGC-3' |

was determined by Bradford assay kit (Sigma, USA) and then the enzyme activity was done based on the supplier's protocols by employing a microplate reader.

2.14. Statistical analysis

All data were reported as mean \pm standard deviation (SD) of five independent experiments. The statistical analyses were done with One-Way ANOVA, Dunnett post-hoc test by using SPSS statistical software. The outcomes were considered statistically significant at $P < 0.05$.

3. Results

3.1. Characterization of synthesized NiO NPs

The size and morphology of the synthesized NiO NPs were assessed by TEM analysis. Typical TEM image of NiO NPs is exhibited in Fig. 1A. TEM image of the of NiO NPs showed the presence of almost spherical-shaped NPs with uniform NP morphology, although a normal aggregation can be observed. Fig. 1A (inset) shows that the NiO NPs shows a particle size distribution with a range of 20 to 500 nm with a dominant average size (average particle diameter of 100 particles) of about 50 nm. The UV-Vis absorption band of NiO NPs was also used to determine the λ_{\max} of synthesized NPs. It was found that the λ_{\max} of NiO NPs is around 335 nm (Fig. 1B), which is almost in good agreement with previous λ_{\max} reported for synthesized NPs (El-Kemary et al., 2013). Furthermore, the FTIR spectrum of NiO NPs showed strong intensity around 510 cm^{-1} associated with Ni-O bond (Fig. 1C). A broad vibration band around 3455 cm^{-1} was also

detected which is attributed to the stretching of O-H band due to the presence of absorbed water (El-Kemary et al., 2013).

3.2. Kinetic study

We analyzed the aggregation kinetics of α -synuclein by reading ThT fluorescence intensity for 40 h. This method permitted us to explore the acceleration effect of NiO NPs on α -synuclein fibrillation. Also, the activity of NiO NPs able to significantly increase the final intensity of ThT and affect the nucleation or elongation rates of the amyloid fibrillation was further investigated with TEM analysis at 40 h. The incubation of 50 μM of α -synuclein aged for 40 h in an aggregation buffer with or without 10 $\mu\text{g/ml}$ NiO NPs exhibited that the NPs accelerated the protein amyloid formation, increasing the induction of ThT positive conformations at 40 h by 52% (Fig. 2). The analysis of the kinetics parameters demonstrated a significant increase in the k_b in presence of NiO NPs ($k_b = 0.057 \pm 0.023$) in comparison with the control sample ($k_b = 0.0034 \pm 0.00019$). The k_a was also higher in the NiO NPs-co-incubated sample ($k_a = 0.49 \pm 0.037 \text{ h}^{-1}$) than in the control sample ($k_a = 0.27 \pm 0.029 \text{ h}^{-1}$). TEM analysis also corroborated that the α -synuclein sample aged for 40 h in an aggregation buffer with NiO NPs contained more fibril products per field than the non-treated sample [Fig. 2 (inset)].

3.3. CR adsorption study

Further analysis of the acceleration effect of NiO NPs on α -synuclein amyloid formation was confirmed by CR absorption assay. It was seen that α -synuclein monomer shows a normalized absorbance of 0.29 at λ_{\max} of 481 nm (Fig. 3). However,

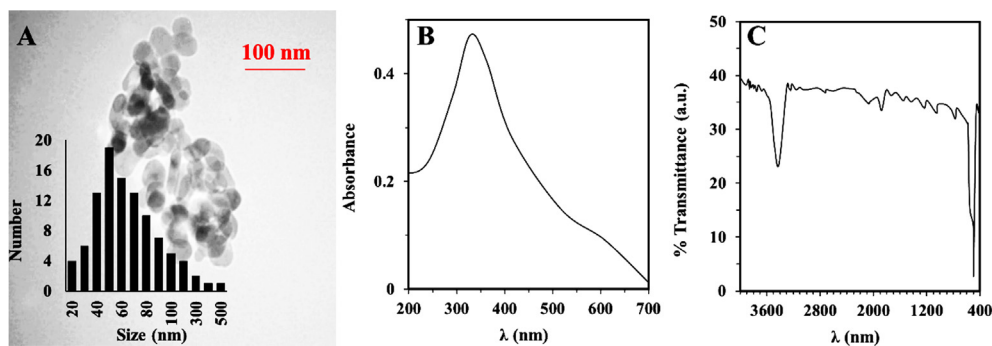


Fig. 1 Characterization of NiO NPs. (A) TEM image, UV-vis adsorption (B), FTIR (C) analysis of synthesized NiO NPs through thermal decomposition method.

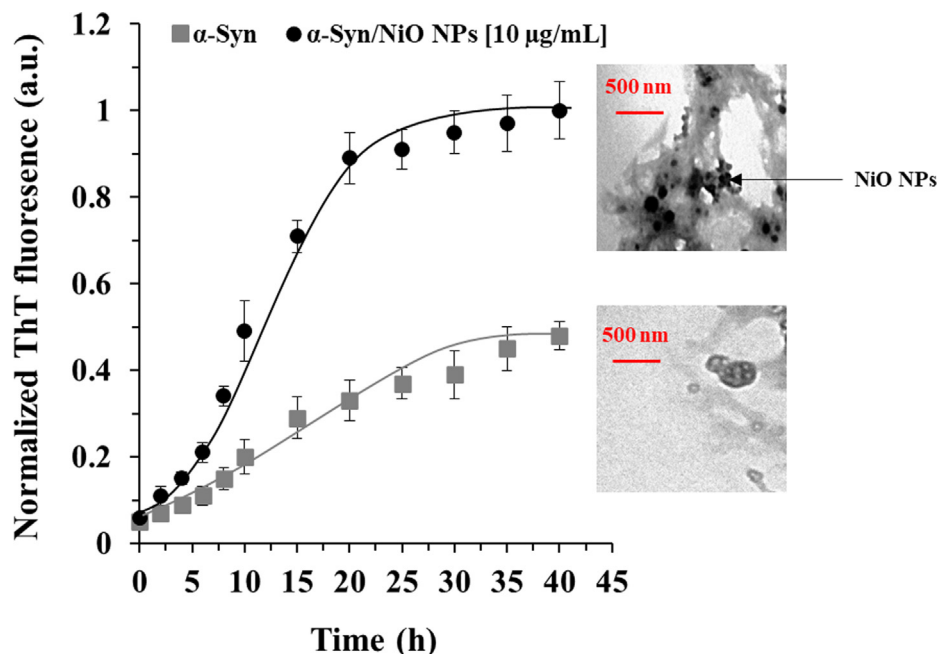


Fig. 2 Kinetic study of protein aggregation with or without NiO NPs. Effects of NiO NPs on the kinetics of α -synuclein amyloid fibrillization as detected by ThT fluorescence experiment. α -Synuclein (50 μ M) was incubated in an aggregation buffer (PBS, pH 7.4, 37 $^{\circ}$ C) and stirred at 100 rpm for 40 h either alone or with a fixed concentration of NiO NPs (10 μ L). TEM images also show the formation of amyloid fibrils taken after 40 h.

CR absorbance was increased in the presence of α -synuclein amyloid alone and α -synuclein/NiO NPs along with a significant red shift (Fig. 3). Also, it was shown the increment rate of absorbance and red shift was higher for α -synuclein samples aged for 40 h with NiO NPs relative to α -synuclein samples at similar condition without NiO NPs (Fig. 3).

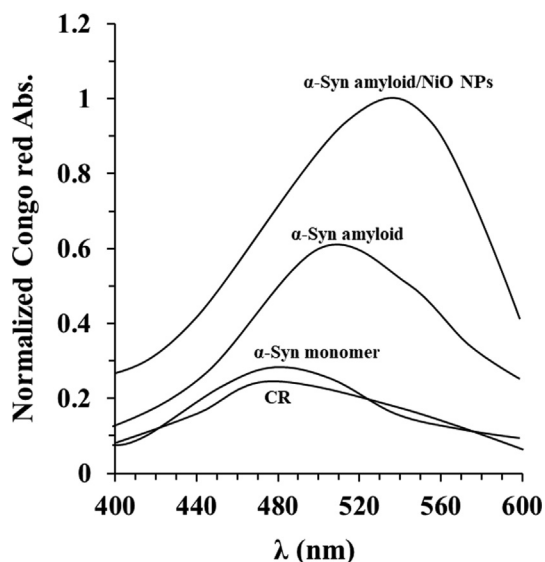


Fig. 3 Congo red absorption of protein aggregation with or without NiO NPs. Congo red adsorption spectra of α -synuclein incubated without or with NiO NPs in the aggregation buffer (PBS, pH 7.4, 37 $^{\circ}$ C) by stirring at 100 rpm for 40 h. Data were reported as explained in Section 2.

3.4. Far-UV-CD study

To explore the α -synuclein secondary structural changes triggered by interaction with NiO NPs or caused by formation of amyloid fibril, far-UV CD spectroscopy was done. Far-UV CD as a sensitive technique can be employed for the investigation of changes in the secondary structure of a biomolecules (23, 24). In agreement with previous studies (Gilan et al., 2019; Khodabandeh et al., 2020; Pang et al., 2021), the far-UV CD band of α -synuclein alone showed one negative minimum at 194 nm, characteristic of random coil proteins (Fig. 4). The changes in α -synuclein secondary structure upon interaction with NiO NPs were rather significant as it follows from significant alterations in the ellipticity and shape of the CD spectrum. Furthermore, upon incubation of α -synuclein at aggregation buffer, far-UV CD spectra also demonstrated dramatic alterations which were more significant in the presence of NiO NPs. In fact, minimum at 194 nm was disappeared and a new minimum appeared at higher wavelength, suggesting the formation of α -helix and β -sheet rich conformations (Gilan et al., 2019; Khodabandeh et al., 2020 Jul; Pang et al., 2021). Exceedingly, upon incubation with NiO NPs, the shape of the far-UV CD of α -synuclein spectra was typical of β -sheet rich conformation, which the ellipticity at 218 nm was increased. These data indicated that NiO NPs accelerated the formation of amyloid fibrils by increasing the formation of β -sheet rich conformations, through destabilizing the native random coil state.

3.5. MTT assay

As depicted in Fig. 5, NiO NPs and α -synuclein amyloid aged for 40 h both in the absence and presence of NiO NPs inhibited

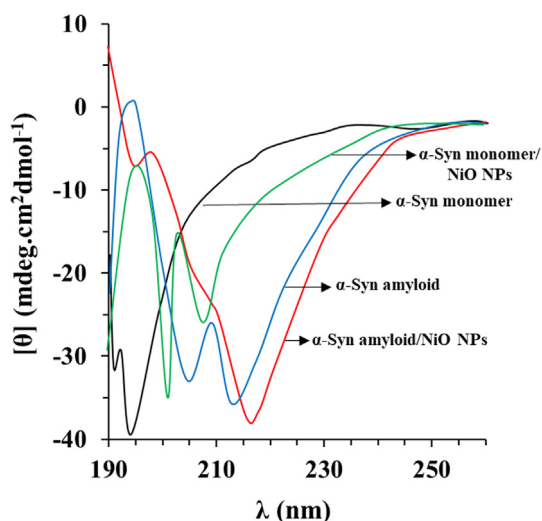


Fig. 4 Far-UV CD study of protein aggregation with or without NiO NPs. CD spectra of α -synuclein incubated without or with NiO NPs in the aggregation buffer (PBS, pH 7.4, 37 °C) by stirring at 100 rpm for 40 h. Data were reported as explained in Section 2.

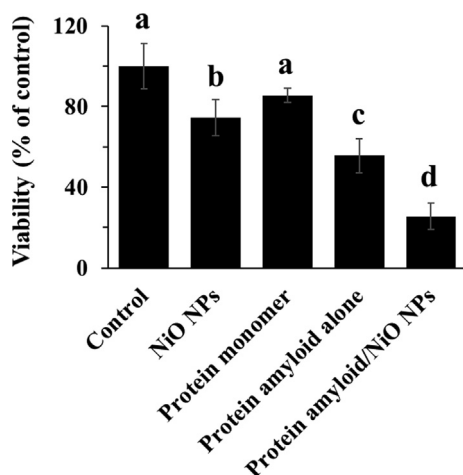


Fig. 5 Cytotoxicity of NiO NPs, α -synuclein monomer, α -synuclein amyloid alone or α -synuclein amyloid in the presence of NiO NPs for 24 h in EOC 13.31 mouse microglia cell line. The cells were incubated with NiO NPs (2 μ g/ml), α -synuclein monomer (10 μ M), α -synuclein amyloid alone (10 μ M), or α -synuclein amyloid (10 μ M) in the presence of NiO NPs (2 μ g/ml) for 24 h and cell viability was assessed by the MTT assay. The data were reported as percentage of microglia cell viability in negative control cells and each value represents the mean \pm SD ($n = 5$). The letters show significantly different from respective defined groups.

the growth of the cells after 24 h. Interestingly, it was seen that the cytotoxic effect of α -synuclein amyloid aged for 40 h in the presence of NiO NPs was more pronounced than those in the absence of NiO NPs or the cells treated only with NiO NPs.

3.6. The expression of inflammatory and apoptosis markers

Inflammation and subsequent apoptosis may be considered as one of the major causes of cell growth inhibition (Angajala and Radhakrishnan, 2014; Cho et al., 2020). Consequently, we explored the expression levels of TNF- α mRNA (Fig. 6A), IL-1 β mRNA (Fig. 6B), IL-6 mRNA (Fig. 6C), Bax mRNA (Fig. 6D), Bcl-2 mRNA (Fig. 6E), and caspase-3 mRNA (Fig. 6F), to determine the induction of inflammation and apoptosis in in EOC 13.31 mouse microglia cell line treated with NiO NPs, α -synuclein monomer, α -synuclein amyloid alone or α -synuclein amyloid in the presence of NiO NPs for 24, as determined by qRT-PCR assay. As indicated in Fig. 6, α -synuclein amyloid monomers induced negligible inflammation and apoptosis. An increase in TNF- α mRNA (Fig. 6A), IL-1 β mRNA (Fig. 6B), IL-6 mRNA (Fig. 6C), Bax mRNA (Fig. 6D), and caspase-3 mRNA (Fig. 6F) was detected in the α -synuclein amyloid- treated cells. Furthermore, α -synuclein amyloid aged for 40 h in the presence of NiO NPs significantly enhanced α -synuclein amyloid -induced inflammation and apoptosis over that of α -synuclein amyloid alone in EOC 13.31 mouse microglia cell line. Also, as shown in Fig. 6E, exposure to the α -synuclein amyloid aged for 40 h in the presence of NiO NPs led to less level of Bcl-2 mRNA than that of α -synuclein alone in in EOC 13.31 mouse microglia cell line. Taken together, these data indicated that NiO NPs greatly enhanced α -synuclein amyloid -induced inflammation of apoptosis in EOC 13.31 mouse microglia cell line.

3.7. Oxidative stress assay

We determined alterations in intracellular ROS level (Fig. 7A), SOD activity (Fig. 7B), and CAT activity (Fig. 7C). The cells were treated with NiO NPs, α -synuclein monomer, α -synuclein amyloid alone or α -synuclein amyloid in the presence of NiO NPs for 24 h, and then cell analysis was done. As shown in Fig. 7A, the production of ROS was significantly increased in cells treated with the NiO NPs, α -synuclein amyloid alone or α -synuclein amyloid in the presence of NiO NPs for 24 h. The fold changes in ROS levels between the negative treated cells as control cells and the cells incubated with NiO NPs, α -synuclein monomer, α -synuclein amyloid alone, or α -synuclein amyloid in the presence of NiO NPs for 24 h were 2.2, 1.56, 3.25 and 7.36, respectively, in EOC 13.31 mouse microglia cell line. The ROS production for the α -synuclein amyloid in the presence of NiO NPs were significantly increased in cells. These data were also verified by SOD (Fig. 7B) and CAT (Fig. 7C) activity assays, indicated that the α -synuclein amyloid in the presence of NiO NPs decreased SOD and CAT activity to induce inflammation and apoptosis more than that of the α -synuclein amyloid in the absence of NiO NPs.

4. Discussion

This study allowed us to indicate that fabricated NiO NPs by thermal decomposition with a size of around 50 nm can accelerate the aggregation of α -synuclein and associated neurotoxicity through upregulation of inflammatory and apoptotic mediators triggered by ROS.

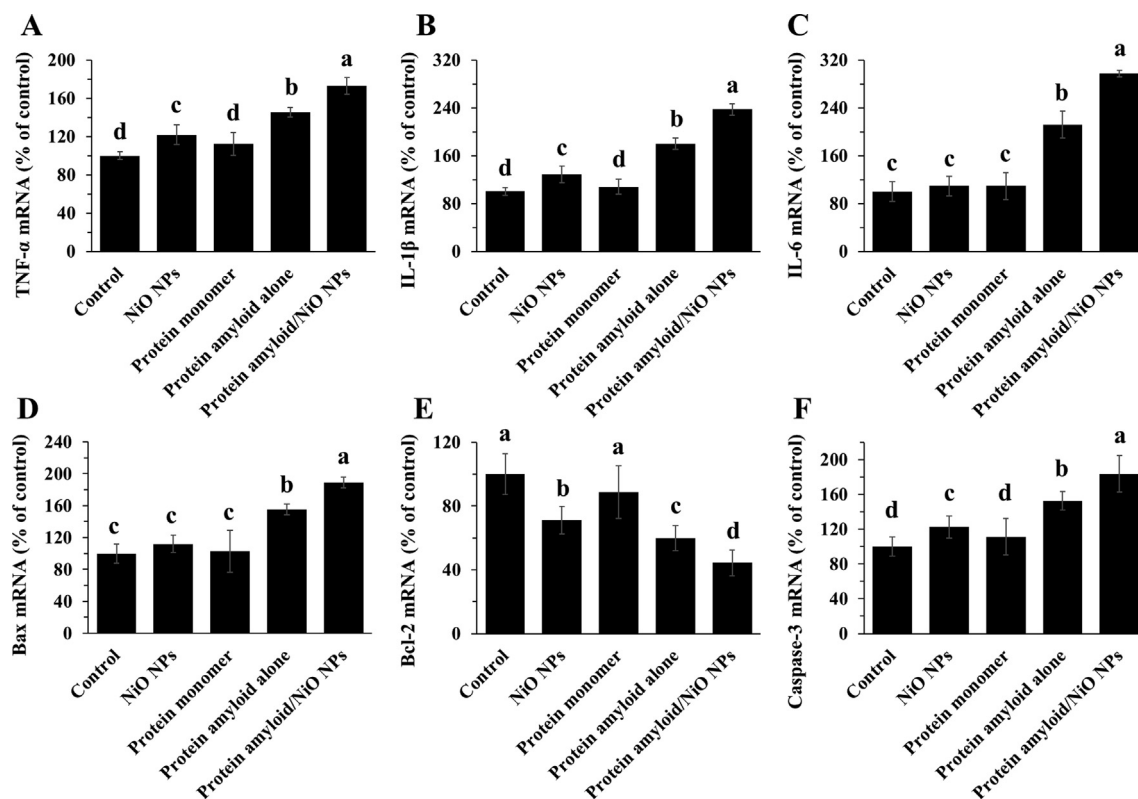


Fig. 6 The expression of inflammatory mediators in EOC 13.31 mouse microglia cell line after incubation with NiO NPs, α -synuclein monomer, α -synuclein amyloid alone or α -synuclein amyloid in the presence of NiO NPs for 24. The cells were incubated with NiO NPs (2 μ g/ml), α -synuclein monomer (10 μ M), α -synuclein amyloid alone (10 μ M), or α -synuclein amyloid (10 μ M) in the presence of NiO NPs (2 μ g/ml) for 24 h and the expression levels of TNF- α mRNA (A), IL-1 β mRNA (B), IL-6 mRNA (C), Bax mRNA (D), Bcl-2 mRNA (E), caspase-3 mRNA (F) were assessed by qRT-PCR. The data were reported as percentage of microglia cell mRNA expression in negative control cells and each value represents the mean \pm SD ($n = 5$). The letters show significantly different from respective defined groups.

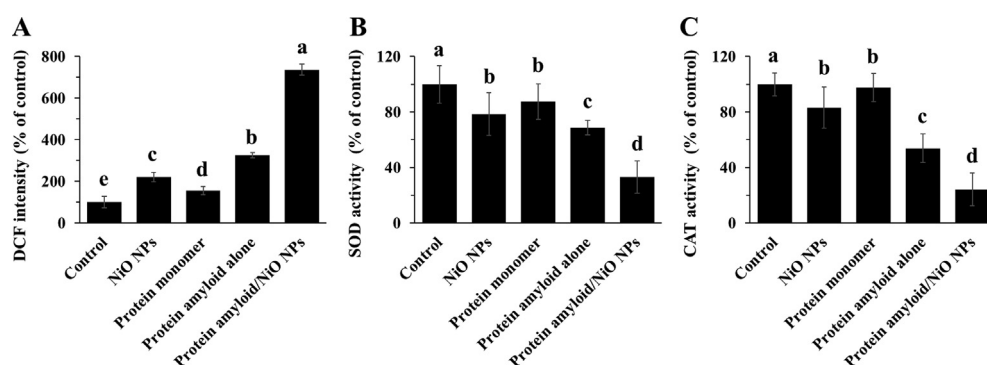


Fig. 7 The evaluation of ROS production and SOD/ CAT activities in EOC 13.31 mouse microglia cell line after incubation with NiO NPs, α -synuclein monomer, α -synuclein amyloid alone or α -synuclein amyloid in the presence of NiO NPs for 24. The cells were incubated with NiO NPs (2 μ g/ml), α -synuclein monomer (10 μ M), α -synuclein amyloid alone (10 μ M), or α -synuclein amyloid (10 μ M) in the presence of NiO NPs (2 μ g/ml) for 24 h and the DCF intensity (A), SOD activity (B), CAT activity (C) was assessed by the methods described in section 2. The data were reported as percentage of microglia cell DCF intensity/SOD, CAT activity in negative control cells and each value represents the mean \pm SD ($n = 5$). The letters show significantly different from respective defined groups.

One of the methods of NP synthesis is thermal decomposition or thermolysis. In this method, a metal-organic precursor, which is an organic-mineral hybrid, typically undergoes irreversible chemical degradation under certain thermal conditions

(Wu et al., 2010; El-Kemary et al., 2013). Due to the conditions applied to the reaction medium, the production of the product can be controlled within the nanoscale range and the desired NPs are synthesized (Wu et al., 2010; El-Kemary

et al., 2013). This method has been extensively used in the preparation of metal oxide magnetic NPs, including NiO NPs (Wu et al., 2010; El-Kemary et al., 2013; Barnett et al., 2018) and iron oxide NPs (Li et al., 2006). In the present study NiO NPs were successfully synthesized through thermal decompaction method and well-characterized by TEM, FTIR and UV-Vis analyses and the data were in good agreement with previous report (El-Kemary et al., 2013).

Afterward, it was seen that NiO NPs can accelerate the formation of α -synuclein amyloid fibrils. It has been documented that although some NPs, including zero valent iron NPs (Gilan et al., 2019), zinc oxide NPs (Khodabandeh et al., 2020), silica NPs (Pang et al., 2021), and gold NPs (Zhang et al., 2009; Álvarez et al., 2013) can induce protein denaturation and subsequent protein aggregation, some other NPs, such as cerium oxide NPs (Zand et al., 2019); graphene oxide sheets (Ghaeidamini et al., 2020), and quantum dot NPs (Ghaeidamini et al., 2020) can inhibit the α -synuclein aggregation. Therefore, it may be concluded that chemical formulation of NPs can play an important role in the inhibition or acceleration of protein aggregation. Also, it has been reported that the effect of NPs on amyloid fibrillization relies on the protein stability and intrinsic amyloid kinetic (Cabaleiro-Lago et al., 2012). Also, it has been shown that the surface functionalization of NPs (Javdani et al., 2019; Taebnia et al., 2015) and the concentration of NPs (Taebnia et al., 2015) can influence the rate of protein aggregation.

Also, it was shown that the significant neurotoxicity of α -synuclein amyloid toward microglia is associated with increased oxidative stress, inflammation and mitochondrial-mediated apoptosis, all of which can be increased by co-incubation of protein samples with NiO NPs.

Oxidative stress as an imbalance between the production of ROS and their elimination by protective mechanisms, can lead to inflammation and apoptosis (Allan, 2002). Indeed, it has been shown that oxidative stress mediated by amyloid proteins can activate various transcription factors, leading to differential expression of some genes involved in inflammatory and apoptotic pathways (Guo et al., 2013). Inflammation caused by oxidative stress is the cause of many neuroadaptive diseases (Deng et al., 2017). Some NPs have been shown to accelerate the protein aggregation and associated neurotoxicity through oxidative stress (Gilan et al., 2019; Khodabandeh et al., 2020; Pang et al., 2021).

It was also shown that α -synuclein amyloids can lead to an elevation of ROS level through a reduction in antioxidant enzymes such as SOD and CAT which leads to disposition of pro-apoptotic proteins (Bax) and anti-apoptotic protein Bcl-2 in the mitochondrial wall and induction of apoptosis (Circu and Aw, 2010). This data indicated that α -synuclein amyloids in the presence of NiO NPs increased the overexpression of Bax and downregulation of Bcl-2 in a more significant manner relative to that of α -synuclein amyloids alone, which can increase oxidative stress-induced apoptosis.

Therefore, further researches should be conducted in the future to explore the inflammatory and oxidative properties of protein amyloids in the presence of NPs. Such data could be important for advances in the treatment of neurodegenerative disorders like Parkinson's disease.

5. Conclusion

Overall, we concluded that the potency of synthesized NiO NPs with a size of around 50 nm in the acceleration, fibrillation and neurotoxicity of α -synuclein amyloid fibrils. It was observed that NiO NPs can disrupt the natively disordered structure or α -synuclein and make it prone to protein aggregation to trigger the overexpression of inflammatory and apoptotic mediators mediated by elevation of ROS. Therefore, our present data could efficiently be useful in the development of metal NPs-based therapeutic platforms for amyloid protein related disease like Parkinson's disease.

Declaration of Competing Interest

The authors declare that they have no known competing financial interests or personal relationships that could have appeared to influence the work reported in this paper.

References

- Allan, B.D., 2002. Amyloid β -peptide (1–42)-induced oxidative stress and neurotoxicity: implications for neurodegeneration in Alzheimer's disease. A review. *Free Radical Res.* 36 (12), 1307–1313.
- Álvarez, Y.D., Fauerbach, J.A., Pellegrotti, J.V., Jovin, T.M., Jares-Erijman, E.A., Stefani, F.D., 2013. Influence of gold nanoparticles on the kinetics of α -synuclein aggregation. *Nano Lett.* 13 (12), 6156–6163.
- Angajala, G., Radhakrishnan, S., 2014. A review on nickel nanoparticles as effective therapeutic agents for inflammation. *Inflammation and Cell Signaling* 1 (3), 1–8.
- Barnett, G.V., Balakrishnan, G., Chennamsetty, N., Meengs, B., Meyer, J., Bongers, J., Ludwig, R., Tao, L., Das, T.K., Leone, A., Kar, S.R., 2018. Enhanced precision of circular dichroism spectral measurements permits detection of subtle higher order structural changes in therapeutic proteins *Oct 1 J. Pharm. Sci.* 107 (10), 2559–2569.
- Cabaleiro-Lago, C., Szczepankiewicz, O., Linse, S., 2012. The effect of nanoparticles on amyloid aggregation depends on the protein stability and intrinsic aggregation rate. *Langmuir* 28 (3), 1852–1857.
- Chaudhary, R.G., Tanna, J.A., Gandhare, N.V., Rai, A.R., Juneja, H. D., 2015. Synthesis of nickel nanoparticles: microscopic investigation, an efficient catalyst and effective antibacterial activity. *Adv. Mater. Lett.* 6 (11), 990–998.
- Cho, Y.L., Tan, H.W., Saquib, Q., Ren, Y., Ahmad, J., Wahab, R., He, W., Bay, B.H., Shen, H.M., 2020. Dual role of oxidative stress-JNK activation in autophagy and apoptosis induced by nickel oxide nanoparticles in human cancer cells. *Free Radical Biol. Med.* 1 (153), 173–186.
- Circu, M.L., Aw, T.Y., 2010. Reactive oxygen species, cellular redox systems, and apoptosis. *Free Radical Biol. Med.* 48 (6), 749–762.
- Cohen, S.I., Vendruscolo, M., Dobson, C.M., Knowles, T.P., 2012. From macroscopic measurements to microscopic mechanisms of protein aggregation. *J. Mol. Biol.* 421 (2–3), 160–171.
- Crespo, R., Villar-Alvarez, E., Taboada, P., Rocha, F.A., Damas, A. M., Martins, P.M., 2016. What can the kinetics of amyloid fibril formation tell about off-pathway aggregation? *J. Biol. Chem.* 291 (4), 2018–2032.
- Croisier, E., Moran, L.B., Dexter, D.T., Pearce, R.K., Graeber, M.B., 2005. Microglial inflammation in the parkinsonian substantia nigra: relationship to alpha-synuclein deposition. *J. Neuroinflammation* 2 (1), 1–8.

- Deng, Y., Long, L., Wang, K., Zhou, J., Zeng, L., He, L., Gong, Q., 2017. Icariside II, a broad-spectrum anti-cancer agent, reverses beta-amyloid-induced cognitive impairment through reducing inflammation and apoptosis in rats. *Front. Pharmacol.* 2 (8), 39.
- El-Kemary, M., Nagy, N., El-Mehasseb, I., 2013. Nickel oxide nanoparticles: synthesis and spectral studies of interactions with glucose. *Mater. Sci. Semicond. Process.* 16 (6), 1747–1752.
- Falahati, M., Attar, F., Sharifi, M., Haertlé, T., Berret, J.F., Khan, R. H., Saboury, A.A., 2019. A health concern regarding the protein corona, aggregation and disaggregation. *Biochim. Biophys. Acta (BBA)-General Subjects* 1863 (5), 971–991.
- Gallardo-Toledo, E., Tapia-Arellano, A., Celis, F., Sinai, T., Campos, M., Kogan, M.J., Sintov, A.C., 2020. Intranasal administration of gold nanoparticles designed to target the central nervous system: fabrication and comparison between nanospheres and nanoprisms. *Int. J. Pharm.* 30 (590), 119957. Nov.
- Gamasae, N.A., Muhammad, H.A., Tadayon, E., Ale-Ebrahim, M., Mirpour, M., Sharifi, M., Salihi, A., Shekha, M.S., Alasady, A.A., Aziz, F.M., Akhtari, K., 2020. The effects of nickel oxide nanoparticles on structural changes, heme degradation, aggregation of hemoglobin and expression of apoptotic genes in lymphocytes. *J. Biomol. Struct. Dyn.* 38 (12), 3676–3686.
- Ghaeidamini, M., Bernson, D., Sasanian, N., Kumar, R., Esbjörner, E.K., 2020. Graphene oxide sheets and quantum dots inhibit α -synuclein amyloid formation by different mechanisms. *Nanoscale*. 12 (37), 19450–19460.
- Gilan, S.S., Rayat, D.Y., Mustafa, T.A., Aziz, F.M., Shahpasand, K., Akhtari, K., Salihi, A., Abou-Zied, O.K., Falahati, M., 2019. α -synuclein interaction with zero-valent iron nanoparticles accelerates structural rearrangement into amyloid-susceptible structure with increased cytotoxic tendency. *Int. J. Nanomed.* 14, 4637.
- Guo, L.L., Guan, Z.Z., Huang, Y., Wang, Y.L., Shi, J.S., 2013. The neurotoxicity of β -amyloid peptide toward rat brain is associated with enhanced oxidative stress, inflammation and apoptosis, all of which can be attenuated by scutellarin. *Exp. Toxicol. Pathol.* 65 (5), 579–584.
- Gustot, A., Gallea, J.I., Sarroukh, R., Celej, M.S., Ruyschaert, J.M., Raussens, V., 2015. Amyloid fibrils are the molecular trigger of inflammation in Parkinson's disease. *Biochem. J.* 471 (3), 323–333.
- Hosseinali, S.H., Boushehri, Z.P., Rasti, B., Mirpour, M., Shahpasand, K., Falahati, M., 2019. Biophysical, molecular dynamics and cellular studies on the interaction of nickel oxide nanoparticles with tau proteins and neuron-like cells. *Int. J. Biol. Macromol.* 15 (125), 778–784.
- Javdani, N., Rahpeyma, S.S., Ghasemi, Y., Raheb, J., 2019. Effect of superparamagnetic nanoparticles coated with various electric charges on α -synuclein and β -amyloid proteins fibrillation process. *Int. J. Nanomed.* 14, 799.
- Khodabandeh, A., Yakhchian, R., Hasan, A., Paray, B.A., Shahi, F., Rasti, B., Mirpour, M., Sharifi, M., Derakhshankhah, H., Akhtari, K., Zhang, Z., 2020. Silybin as a potent inhibitor of α -synuclein aggregation and associated cytotoxicity against neuroblastoma cells induced by zinc oxide nanoparticles. *J. Mol. Liq.* 15 (310), Jul 113198.
- Koo, E.H., Lansbury, P.T., Kelly, J.W., 1999. Amyloid diseases: abnormal protein aggregation in neurodegeneration. *Proc. Natl. Acad. Sci.* 96 (18), 9989–9990.
- Li, X., Zhang, X., Li, Z., Qian, Y., 2006 Jan 1. Synthesis and characteristics of NiO nanoparticles by thermal decomposition of nickel dimethylglyoximate rods. *Solid State Commun.* 137 (11), 581–584.
- Mehra, S., Sahay, S., Maji, S.K., 2019. α -Synuclein misfolding and aggregation: Implications in Parkinson's disease pathogenesis. *Biochim. Biophys. Acta (BBA)-Proteins and Proteomics* 1867 (10), 890–908.
- Nakhjiri, M.Z., Asadi, S., Hasan, A., Babadaei, M.M., Vahdani, Y., Rasti, B., Ale-Ebrahim, M., Arsalan, N., Goorabjavari, S.V., Haghghat, S., Sharifi, M., 2020. Exploring the interaction of synthesized nickel oxide nanoparticles through hydrothermal method with hemoglobin and lymphocytes: Bio-thermodynamic and cellular studies. *J. Mol. Liq.* 1 (317), 113893. Nov.
- Pang, C., Zhang, N., Falahati, M., 2021. Acceleration of α -synuclein fibril formation and associated cytotoxicity stimulated by silica nanoparticles as a model of neurodegenerative diseases. *Int. J. Biol. Macromol.* 1 (169), 532–540.
- Taebnia, N., Morshedi, D., Doostkam, M., Yaghmaei, S., Aliakbari, F., Singh, G., Arpanaei, A., 2015. The effect of mesoporous silica nanoparticle surface chemistry and concentration on the α -synuclein fibrillation. *RSC Adv.* 5 (75), 60966–60974.
- Wang, W., Nema, S., Teagarden, D., 2010. Protein aggregation—pathways and influencing factors. *Int. J. Pharm.* 390 (2), 89–99.
- Wu, Z.G., Munoz, M., Montero, O., 2010 Mar 1. The synthesis of nickel nanoparticles by hydrazine reduction. *Adv. Powder Technol.* 21 (2), 165–168.
- Zand, Z., Khaki, P.A., Salihi, A., Sharifi, M., Nanakali, N.M., Alasady, A.A., Aziz, F.M., Shahpasand, K., Hasan, A., Falahati, M., 2019. Cerium oxide NPs mitigate the amyloid formation of α -synuclein and associated cytotoxicity. *Int. J. Nanomed.* 14, 6989.
- Zhang, D., Neumann, O., Wang, H., Yuwono, V.M., Barhoumi, A., Perham, M., Hartgerink, J.D., Wittung-Stafshede, P., Halas, N.J., 2009. Gold nanoparticles can induce the formation of protein-based aggregates at physiological pH. *Nano Lett.* 9 (2), 666–671.